Dissecting how ALS-associated D290V mutation enhances pathogenic aggregation of $hnRNPA2_{286\text{-}291}$ peptides: dynamics and conformational ensembles

Yuan Tan, Yujie Chen, Xianshi Liu, Yiming Tang, Zenghui Lao, and Guanghong Wei**

Department of Physics, Fudan University, Shanghai 200438, People's Republic of China.

1 | Introduction

The aggregation of RNA binding proteins, including hnRNPA1/2, TDP-43 and FUS, is heavily implicated in causing or increasing disease risk for a series of neurodegenerative diseases such as amyotrophic lateral sclerosis (ALS) [1]. A recent experimental study [2] demonstrated that an ALS-related D290V mutation in the low complexity domain (LCD) of hnRNPA2 can enhance the aggregation propensity of wild type (WT) $hnRNPA2_{286\text{-}291}$ peptide. However, the underlying molecular mechanisms remain elusive. Herein, we investigated effects of D290V mutation on aggregation dynamics of $hnRNPA2_{286\text{-}291}$ peptide and the conformational ensemble of $hnRNPA2_{286\text{-}291}$ oligomers by performing all-atom molecular dynamic (MD) and replica-exchange molecular dynamic (REMD) simulations.

2 | Results

- **D290V mutation reduces the fluidity of $hnRNPA2_{286\text{-}291}$ peptide and increases the stability of $hnRNPA2_{286\text{-}291}$ oligomers in MD simulations.**

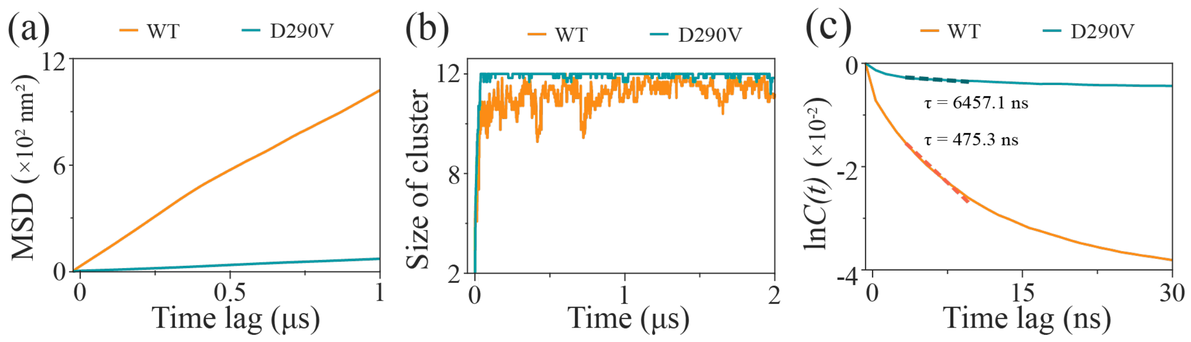

Fig. 1. (a) The MSD as a function of the time lag. (b) The time evolution of the size of largest cluster. (c) The decay of correlation function for the largest cluster in the WT/D290V systems.

- **REMD simulations show that D290V mutation significantly increases the β-sheet propensity and ordering of $hnRNPA2_{286\text{-}291}$ oligomers.**

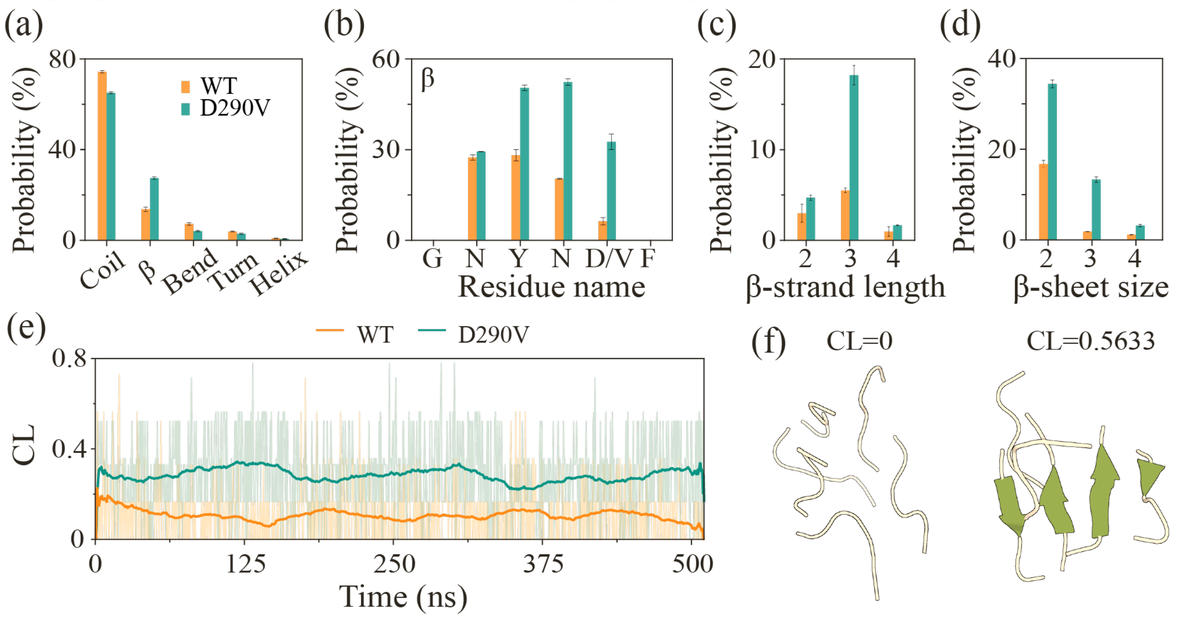

Fig. 2. (a) Probability of each secondary structure (including coil, β-structure, bend, turn and helix). (b) β-sheet probability of each amino acid residue. (c) Probability of β-strand length. (d) Probability of different sizes of β-sheets. (e) Time evolution of CL values of WT and D290V $hnRNPA2_{286\text{-}291}$ oligomer. (f) Representative snapshots when CL are 0 and 0.5633.

- **D290V mutation alters the free energy landscape of $hnRNPA2_{286\text{-}291}$ oligomers.**

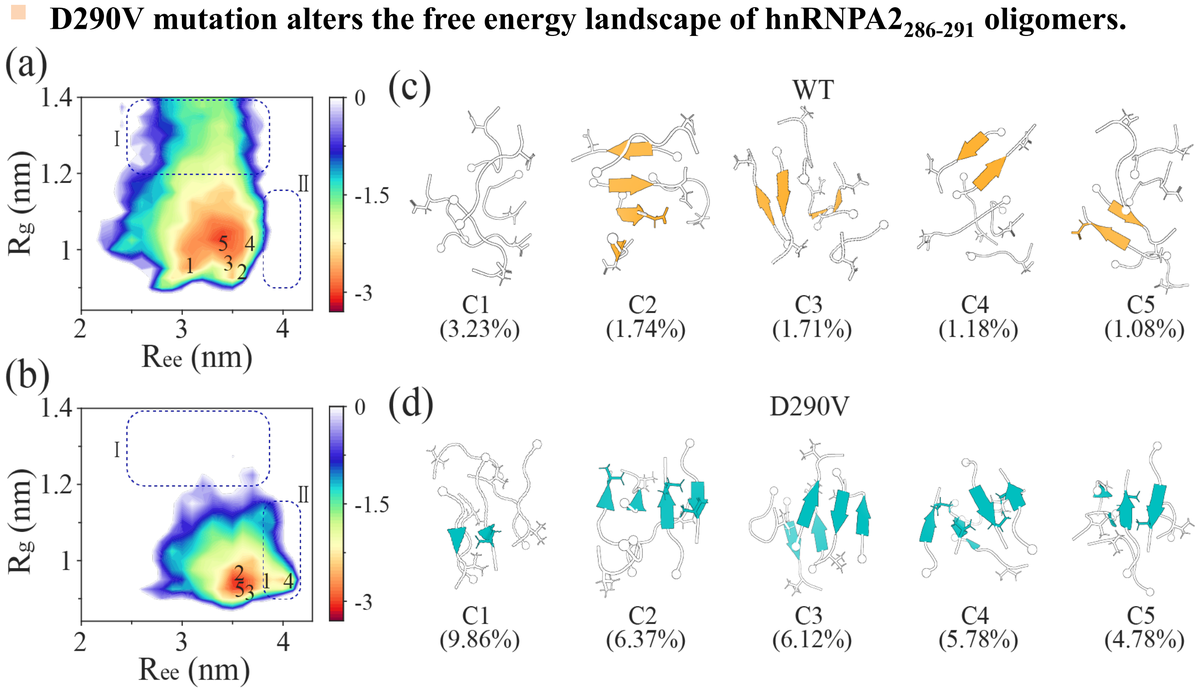

Fig. 3. (a-b) PMFs (in kcal/mol) as a function of Rg and Ree. (c-d) Representative conformations for the five most-populated clusters along with their corresponding populations of (c) WT and (b) D290V $hnRNPA2_{286\text{-}291}$ oligomers. Their locations are labeled on the PMF plots.

- **D290V $hnRNPA2_{286\text{-}291}$ oligomers exhibit stronger interchain interactions including hydrophobic and hydrogen-bonding interactions than WT.**

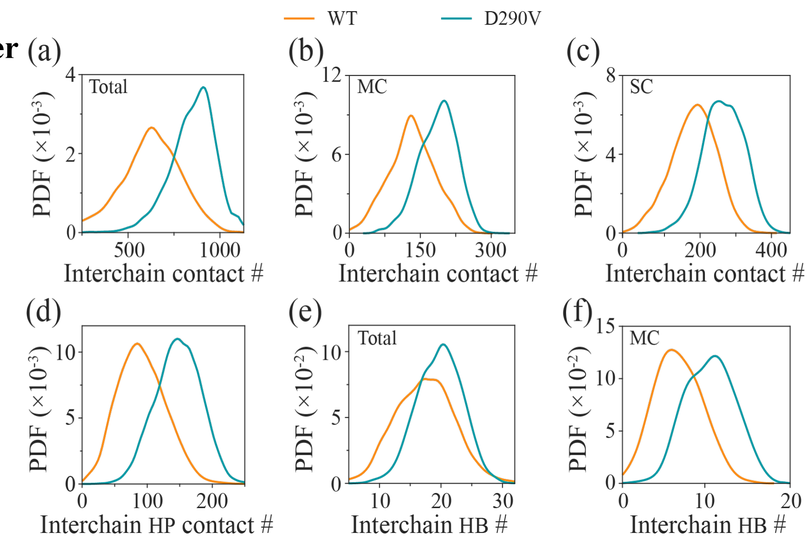

Fig. 4. PDFs of (a) total contact number, (b) mainchain (MC) contact number, (c) sidechain (SC) contact number, (d) hydrophobic (HP) contact number, (e) total hydrogen bond (HB) number, and (f) MC HB number in WT/D290V oligomers.

- **D290V mutation strengthens hydrophobic interactions between residue 290 and Y288/V290/F291, along with main chain hydrogen bonding interactions of Y288-V290 and N287-N289 residue pairs, which induces formation of parallel β-sheets.**

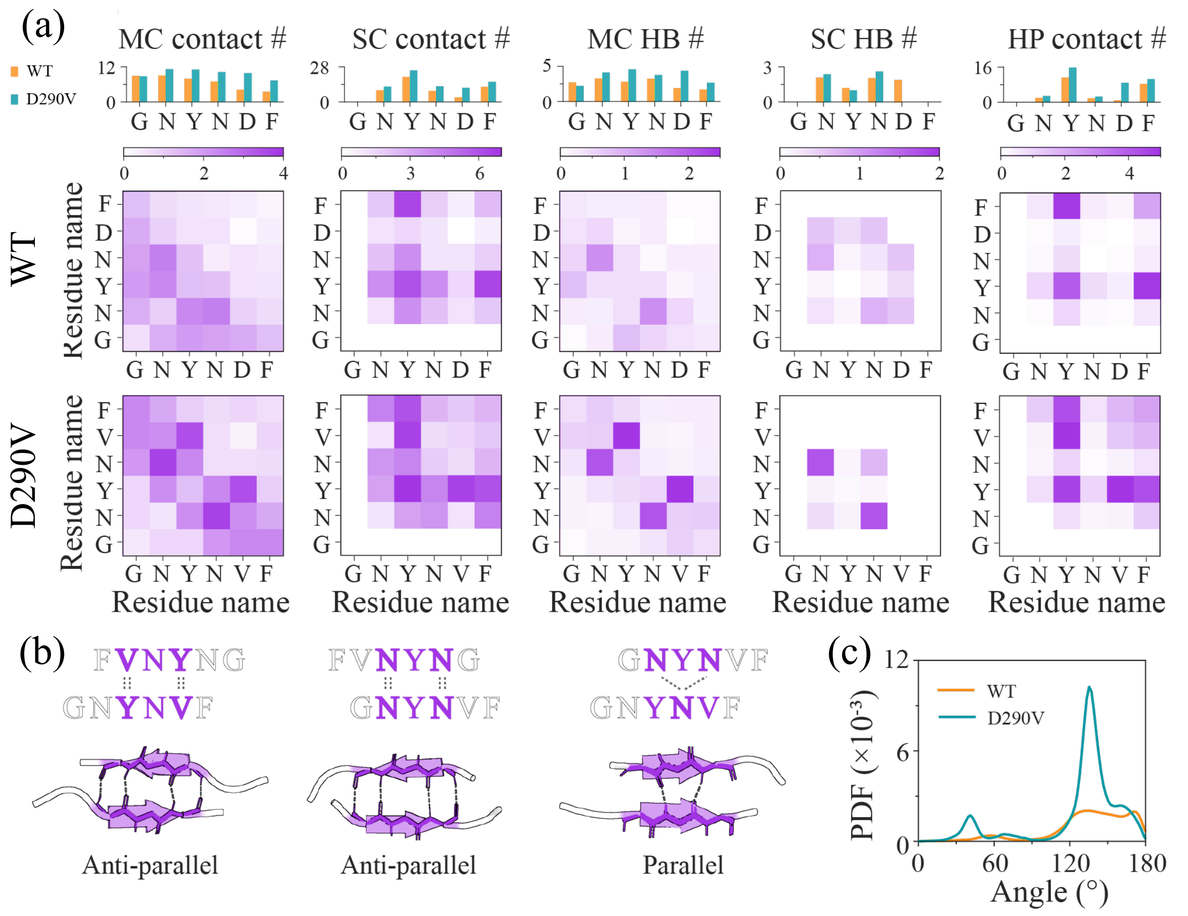

Fig. 5. Impact of D290V mutation on pairwise residue–residue interaction and β-sheet patterns of $hnRNPA2_{286\text{-}291}$ oligomers. Maps of (a) MC contact number, SC contact number, MC HB number, SC HB number, and HP contact number. Bar charts above the maps show the cumulative contact numbers between each residue and other residues. (b) Representative snapshots of anti-parallel and parallel β-sheets. The black dashed lines indicate Y288-V290/N287-N289 hydrogen bonds. (c) PDF of angles between two strands in all β-sheets of WT and D290V $hnRNPA2_{286\text{-}291}$ oligomers.

- **D290V oligomers display stronger Y288–Y288 aromatic interaction than WT.**

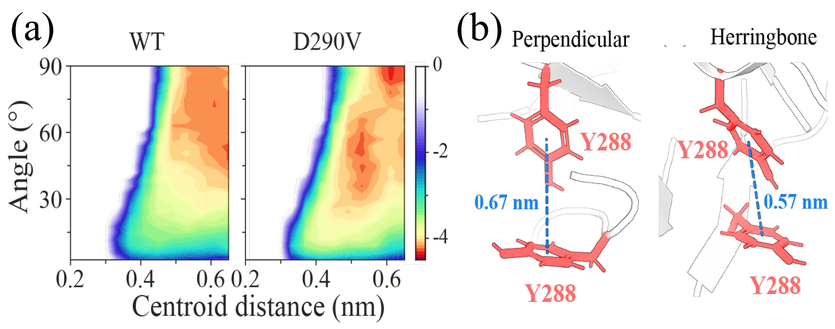

Fig. 6. (a) PMFs (in kcal/mol) of two aromatic rings and the angle of the two rings, with two rings from Y288 and Y288 in WT and D290V systems. Representative snapshots of (b) perpendicular and herringbone π-π stacking.

3 | Conclusions

Our simulations demonstrate that D290V mutation greatly reduces the dynamics of $hnRNPA2_{286\text{-}291}$ peptide and that D290V oligomers possess higher compactness and β-sheet content than WT, indicative of mutation-enhanced aggregation capability. Specifically, D290V mutation strengthens inter-peptide hydrophobic, main-chain hydrogen bonding and side-chain aromatic stacking interactions. Those interactions collectively lead to the enhancement of aggregation capability of $hnRNPA2_{286\text{-}291}$ peptides. Overall, our study provides insights into the dynamics and thermodynamic mechanisms underlying D290V-induced disease-causing aggregation of $hnRNPA2_{286\text{-}291}$, which could contribute to better understanding of the transitions from reversible condensates to irreversible pathogenic aggregates of hnRNPA2 LCD in ALS-related diseases.

4 | References

[1] Kim, Hong Joo, et al. Mutations in prion-like domains in hnRNPA2B1 and hnRNPA1 cause multisystem proteinopathy and ALS. *Nature* 495.7442 (2013): 467.

[2] Lu, Jiahui, et al. CryoEM structure of the low-complexity domain of hnRNPA2 and its conversion to pathogenic amyloid. *Nature communications* 11.1 (2020): 4090.